Molecular Pharmacology Fast Forward. Published on December 9, 2014 as DOI: 10.1124/mol.114.095539
This article has not been copyedited and formatted. The final version may differ from this version.

Neurotransmitter GABA activates muscle but not α7 nicotinic receptors

Leonardo Dionisio, Ignacio Bergé, Matías Bravo, María del Carmen Esandi and Cecilia Bouzat

Instituto de Investigaciones Bioquímicas de Bahía Blanca, UNS-CONICET, Camino La Carrindanga Km7, 8000 Bahía Blanca, Argentina[1]

[1]

Molecular Pharmacology Fast Forward. Published on December 9, 2014 as DOI: 10.1124/mol.114.095539
This article has not been copyedited and formatted. The final version may differ from this version.

Running title: GABA actions at nAChRs

Corresponding author: Cecilia Bouzat. Instituto de Investigaciones Bioquímicas de Bahía Blanca. Camino La Carrindanga Km 7. 8000 Bahia Blanca. Argentina. E-mail: inbouzat@criba.edu.ar. Telephone: 54-291-4861201- FAX: 54-291-4861200

Number of text pages: 29

Number of *Tables*: 1

Number of *Figures*: 5

Number of *References*: 63

Number of words in the *Abstract:* 247

Number of words in the *Introduction*: 639

Number of words in the *Discussion:* 1384

Abbreviations: nAChR, nicotinic acetylcholine receptor; ACh, acetylcholine; $5HT_3A$, serotonin receptor type 3A; α-BTX, α-bungarotoxin; AChBP, Acetylcholine binding protein; ms, millisecond; min, minute; BBE, best binding energy.

Molecular Pharmacology Fast Forward. Published on December 9, 2014 as DOI: 10.1124/mol.114.095539
This article has not been copyedited and formatted. The final version may differ from this version.

Abstract

Cys-loop receptors are neurotransmitter-activated ion channels involved in synaptic and extrasynaptic transmission in the brain and are also present in non-neuronal cells. As $GABA_A$ and nicotinic receptors (nAChR) belong to this family, we explored by macroscopic and single-channel recordings if the inhibitory neurotransmitter GABA has the ability to activate excitatory nAChRs. GABA differentially activates nAChR subtypes. It activates muscle nAChRs, with maximal peak currents of about 10 % of those elicited by ACh and 15-fold higher EC50 with respect to ACh. At the single-channel level, the weak agonism is revealed by the requirement of 20-fold higher concentration of GABA for detectable channel openings, a major population of brief openings, and absence of clusters of openings when compared to ACh. Mutations at key residues of the principal binding-site face of muscle nAChRs (αY190 and αG153) affect GABA-activation similarly as ACh-activation whereas a mutation at the complementary face (εG57) shows a selective effect for GABA. Studies with subunit-lacking receptors show that GABA can activate muscle nAChRs through the α/δ interface. Interestingly, single-channel activity elicited by GABA is similar to that elicited by ACh in gain-of-function nAChR mutants associated to congenital myasthenic syndromes, which could be important in the progression of the disorders due to steady exposure to serum GABA. In contrast, GABA cannot elicit single-channel or macroscopic currents of α7 or the chimeric α7-$5HT_3A$ receptor, a feature important for preserving an adequate excitatory/inhibitory balance in the brain as well as for avoiding activation of non-neuronal receptors by serum GABA.

Molecular Pharmacology Fast Forward. Published on December 9, 2014 as DOI: 10.1124/mol.114.095539
This article has not been copyedited and formatted. The final version may differ from this version.

Introduction

Nicotinic acetylcholine receptors (nAChR) are members of the Cys-loop ligand-gated ion channel superfamily that also includes glycine, serotonin-type 3 ($5\text{-}HT_3A$), and $GABA_A$ receptors (Bouzat, 2012). α7 nAChRs are among the most abundant in the central nervous system. They contribute to cognitive functioning, sensory information processing, attention, working memory, and reward pathways. Decline or alterations of signaling involving α7 have been implicated in neurological diseases, such as schizophrenia, epilepsy, autism and Alzheimer's disease (Hurst et al., 2013; Thomsen et al., 2010; Wallace and Porter, 2011; Wallace and Bertrand, 2013; Kalamida et al., 2007). α7 nAChRs localize both pre- and post-synaptically, but they dominantly operate in an extra-synaptic mode (Lendvai and Vizi, 2008). Volume transmission is also relevant in non-neuronal cells, such as lymphocytes and macrophages where α7 is involved in anti-inflammatory responses (Andersson and Tracey, 2012; De Rosa et al., 2009). Muscle nAChRs are confined at post-synaptic locations in muscle fibers and are mainly implicated in myasthenia gravis and congenital myasthenic syndromes (Engel et al., 2012).

nAChR subunits are classified as either α, which contain a disulfide bridge important for acetylcholine (ACh) binding, or non-α subunits, which lack this motif (Matsuda et al., 2005). nAChRs assemble from five identical α subunits, such as α7, or from different α and non-α subunits, such as the muscle nAChR, which in the adult is composed of two α1, one β, one δ and one ε subunits. The five homologous subunits are arranged as barrel staves around a central ion-conducting pore (Bartos et al., 2009). Approximately half of each subunit is extracellular with the remainder comprising transmembrane domains M1-M4 and a large cytoplasmic domain spanning M3 and M4 (Bouzat, 2012). The neurotransmitter binding sites are formed within the extracellular domain at interfaces between subunits (Sine et al., 2002). One of the sides, called the principal face, is formed by three discontinuous loops of the α subunit whereas the

Molecular Pharmacology Fast Forward. Published on December 9, 2014 as DOI: 10.1124/mol.114.095539
This article has not been copyedited and formatted. The final version may differ from this version.

complementary face is formed by three discontinuous β-strands of the adjacent subunit, which in the muscle nAChR is either the ε or the δ subunit. Key residues of the principal face are grouped in regions called Loops A, B and C, at the principal face and Loops D, E and F at the complementary face (Sine and Engel, 2006), (Brejc et al., 2001), (Nys et al., 2013). Residues of the principal face are highly conserved between α7 and α1 subunits, whereas less conservation is found in residues located at the complementary face (Bartos et al., 2009). The potential for understanding ligand binding at the atomic structural level arose with the discovery of acetylcholine-binding protein (AChBP) (Brejc et al., 2001), a soluble protein homologous to the ligand binding domains of pentameric ligand-gated ion channels. Homology models from AChBP have helped to gain in-depth understanding of how ligands bind to an ACh binding site.

GABA is the main inhibitor neurotransmitter in the nervous system and can exert its effects through $GABA_A$ receptors located at inhibitory synapses. However, GABA released at the synaptic cleft can diffuse and reach receptors outside of the synapse, on the soma, dendrites and axon (Kullmann et al., 2005). Thus, GABA can be involved in both synaptic and extra-synaptic actions in the brain (Olah et al., 2009). Moreover, GABA might even have a broader spectrum of effects since it is also present in blood at a concentration of 0.1 μM (Bjork et al., 2001). Given that $GABA_A$ receptors and nAChRs belong to the same Cys-loop family, we sought to explore if the inhibitory neurotransmitter GABA is able to activate excitatory nAChRs, thus leading to cross-talk among family members. To this end, we evaluated the action of GABA at the neuronal α7 and muscle nAChR by macroscopic and single-channel recordings. Our results demonstrate that GABA has the ability to activate muscle but not α7 nAChRs and provide insights into the structural and mechanistic differences with respect to ACh activation.

Molecular Pharmacology Fast Forward. Published on December 9, 2014 as DOI: 10.1124/mol.114.095539
This article has not been copyedited and formatted. The final version may differ from this version.

Materials and Methods

Site-directed mutagenesis and expression of α7 and adult muscle nAChR

BOSC 23 cells, which are modified HEK293 cells (Pear et al., 1993), were transfected with wild type or mutant subunit cDNAs of adult muscle nAChRs: α1, β, ε, and δ, human α7 or α7-5HT$_3$A using calcium phosphate precipitation (Bouzat et al., 2002), (Bouzat et al., 2004, Bouzat et al., 2008). To promote receptor expression on the cell surface, the human α7 cDNA was co-transfected with cDNA encoding the chaperone protein RIC-3 (Williams et al., 2005). A plasmid encoding green fluorescent protein was included in all transfections to allow the identification of transfected cells under fluorescence optics. Cells were used for current measurements 48 or 72 h after transfection. Mutant subunits were constructed using the QuikChange site-directed mutagenesis kit (Stratagene).

Patch-clamp experiments

Single-channel recordings

Single-channel currents were recorded in the cell-attached configuration (Hamill et al., 1981) at room temperature. The bath and pipette solutions contained 140 mM KCl, 5.4 mM NaCl, 1.8 mM $CaCl_2$, 1.7 mM $MgCl_2$, and 10 mM HEPES (pH 7.4). For α7-5HT$_3$A the bath solution contained low calcium (0.2 mM) to avoid open-channel block (Bouzat et al., 2008). Currents were recorded using an Axopatch 200 B patch-clamp amplifier (Axon Instruments, Inc., CA), digitized at 5 μs intervals, recorded using the Acquire program (Bruxton Corporation, Seattle, WA), and detected by the half-amplitude threshold criterion using the TAC 4.0.10 program (Bruxton Corporation). Channels were typically recorded at a membrane potential of –70 mV. Open- and closed-time histograms were plotted using a logarithmic abscissa and a square root ordinate and fitted to the sum of exponential functions by maximum likelihood using the TACFit program (Bruxton Corporation). Clusters or bursts of openings corresponding to a

Molecular Pharmacology Fast Forward. Published on December 9, 2014 as DOI: 10.1124/mol.114.095539
This article has not been copyedited and formatted. The final version may differ from this version.

single receptor channel were identified as a series of closely spaced events preceded and followed by closed intervals greater than a specified duration (τ_{crit}); this duration was taken as the point of intersection of the predominant closed time component and the succeeding one in the closed time histogram (Bouzat et al., 2000).

In some experiments, the tip of the pipette was filled with a solution containing ACh or GABA and the shaft with the same solution containing ACh and GABA or GABA and α-BTX. Channel recordings obtained immediately after seal formation were assigned the status of control condition. As with time the shaft solution diffuses to the tip of the pipette, channels recorded 5-6 min after the beginning of the recording were considered the exposed condition. Only patches in which the seal was made rapidly were used for this type analysis.

Whole-cell recordings

Currents were recorded in the whole-cell patch-clamp configuration at a pipette potential of −70 mV at room temperature. The pipette solution contained 134 mM KCl, 5 mM EGTA, 1.7 mM $MgCl_2$, and 10 mM HEPES, pH 7.3. The extracellular solution (ECS) contained 150 mM NaCl, 1.8 mM $CaCl_2$, 1 mM $MgCl_2$ and 10 mM HEPES, pH 7.3. Rapid agonist perfusion was performed as described before (Corradi et al., 2009). Briefly, the perfusion system consisted of solution reservoirs suspended on a pole for gravity-driven flow, switching valves, a solenoid-driven pinch valve, and two tubes oriented into the culture dish. One tube contained ECS without agonist and the other contained ECS with agonist. When the pinch valve was switched, solution flowed from only one side at a time, and switched from one side to the other. This perfusion system allowed for a rapid exchange (0.1 to 1 ms) of the solution bathing the patch. Macroscopic currents were recorded using an Axopatch 200 B patch-clamp amplifier (Axon Instruments, Inc., CA) and filtered at 5 kHz. Data analysis was performed using the IgorPro software (WaveMetrics Inc, Lake Oswego, OR). Current records were aligned at the point at which the current reached 50% of maximum. Peak currents

Molecular Pharmacology Fast Forward. Published on December 9, 2014 as DOI: 10.1124/mol.114.095539
This article has not been copyedited and formatted. The final version may differ from this version.

correspond to the value obtained by extrapolation of the decay current to this point. Current decays were fitted by an exponential decay function:

$$I(t)=I_0\exp(-t/\tau_d)+I_\infty \qquad \text{(Equation 1)}$$

where I_0 and I_∞ are peak and the steady state current values, respectively, and τ_d is the decay time constant (Andersen et al., 2011).

EC50 and Hill coefficient values were calculated by nonlinear regression analysis using the Hill equation:

$$I/I_{max} = 1/[1 + (EC50/L)^{nH}] \qquad \text{(Equation 2)}$$

where EC50 is the agonist concentration that elicits the half-maximal response, n_H is the Hill coefficient, and L is the agonist concentration (Bartos et al., 2006).

Homology modeling and molecular docking

Homology models of the extracellular domain of the human neuronal α7 nAChR and the adult mouse muscle nAChR were created using the structure of the nicotine-bound *Lymnaea stagnalis* acetylcholine binding protein (AChBP; Protein Data Bank code 1UW6) as template. The amino acid sequences were aligned using ClustalW (http://www.ebi.ac.uk/Tools/msa/clustalw2/) and modeling was performed using Modeller 9 v.11 (http://salilab.org/ modeller/) (Sali et al., 1995). We have not included in our analysis Loop F of δ and ε subunits because it cannot be modeled reliably (Arias et al., 2013;Hernando et al., 2012). Symmetry constraints were imposed on the Cα atoms for the same α-type subunit. Ten models were constructed, and the one with the highest Modeller scores and the smallest percentage of amino acids in the disallowed region of the Ramachandran plot was selected for docking studies. ACh or GABA molecules were docked separately into the agonist binding sites located at α−δ, α−ε or each of the five α7−α7 interfaces using AutoDock version 4.3 (Morris et al., 2009). The ligand binding site was defined as being within 20 Å of W149. One hundred genetic algorithm runs were performed for each condition. Clustering of the results was done

Molecular Pharmacology Fast Forward. Published on December 9, 2014 as DOI: 10.1124/mol.114.095539
This article has not been copyedited and formatted. The final version may differ from this version.

with AutoDock based on a root-mean-square deviation cutoff of 2.0 Å. Docking results were corroborated in four different procedures. Best docking poses for each drug and interface were plotted with Discovery Studio Visualizer 3.5 (Accelrys Software Inc.).

Statistics: Experimental data are shown as mean ± S.D. Statistical comparisons were done using the Student's t test. A level of $p<0.05$ was considered significant.

Molecular Pharmacology Fast Forward. Published on December 9, 2014 as DOI: 10.1124/mol.114.095539
This article has not been copyedited and formatted. The final version may differ from this version.

Results

GABA activates muscle nAChRs

To evaluate if the neurotransmitter GABA is able to activate muscle nAChR we first recorded macroscopic currents in the whole-cell configuration from cells transfected with α1, β, δ, and ε subunits. At concentrations higher than 25 μM, GABA elicits macroscopic responses of adult muscle nAChR. Maximal responses elicited by 500 μM GABA are 10.5 ± 3.5 % of those elicited by 500 μM ACh (Fig. 1A). Expressing the relative peak current as a function of agonist concentration results in values of EC50 of 18 ± 1.1 μM (nH= 2.7 ± 0.7, n= 3) and 268 ± 80 μM (nH= 0.7 ± 0.2, n= 3) for ACh and GABA, respectively (Fig. 1A). These results indicate that GABA has the ability to activate muscle nAChRs although it behaves as a very low-efficacy agonist.

To reveal the basis underlying partial activation of muscle nAChR by GABA we performed single-channel recordings (Fig. 1B). Single-channel openings are readily detected at GABA concentrations as low as 1 μM GABA. Activity appears mainly as isolated openings flanked by long closings (Fig. 1B). For GABA concentrations lower than 1 μM, the frequency of openings was markedly low and many patches appeared silent. To unequivocally confirm that the detected channel activity arises from GABA-activated nAChRs and not from endogenous GABA receptors, we recorded single-channels from cells transfected only with GFP cDNA, and in parallel, from cells of the same batch transfected with GFP and nAChR-subunit cDNAs. Whereas no channels are detected in cells expressing GFP alone, nAChR expressing cells show clear single-channel activity in the presence of 1 mM GABA. Also, the mean amplitude of opening events detected from cells expressing muscle nAChR is similar for recordings performed in the presence of 1 mM ACh (5.67 ± 0.06 pA, n=3, -70 mV) or 1 mM GABA (5.61 ± 0.17 pA, n=3, -70 mV).

At all tested GABA concentrations (1 μM-10 mM), open time histograms are fitted by two components (Supplemental Table 1). The duration of the slowest open component is similar to that of ACh-activated channels (~1 ms, Supplemental Table 1,

Molecular Pharmacology Fast Forward. Published on December 9, 2014 as DOI: 10.1124/mol.114.095539
This article has not been copyedited and formatted. The final version may differ from this version.

(Bouzat et al., 2000;Bouzat et al., 2002). In the presence of GABA, the long openings correspond to only 30 % of total openings and the main population of events is composed of brief openings (mean open duration ~100 μs). In contrast, long openings are predominant in the presence of ACh (>75% at 1 μM ACh) (Table 1). At ACh concentrations higher than 10 μM, muscle nAChR opens in clusters of well-defined activation episodes (Fig. 1B, Bouzat et al., 2002)). Each activation episode, named cluster, begins with the transition of a single receptor from the desensitized to the activatable state and terminates by returning to the desensitized state. Closed time histograms for ACh show a main intracluster component that is sensitive to ACh concentration (Bouzat et al., 2000) (Fig. 1B). GABA cannot elicit activation in clusters at any concentration (1 μM-10 mM) (Fig. 1B). Also, closed time histograms do not show a component sensitive to GABA concentration as observed for ACh (Fig. 1B). These results explain why GABA acts as a low-efficacy agonist of muscle nAChR.

We also performed single-channel recordings with a pipette in which the tip was filled with the solution containing 1 mM GABA and the shaft, with the same solution containing 1 mM GABA and 1 μM α-BTX. Single-channel openings were readily detected in the first seconds after seal formation, and then channel activity profoundly decreased as a function of time (Fig. 1C). As a control, we verified that specific labeling of Alexa Fluor 594 α-BTX was not detected in our untransfected cells, in good agreement with previous report in HEK cells (McCann et al., 2006).

This result demonstrates that the detected channel activity arises from nAChR and that GABA-activated channels are blocked by α-BTX.

Activation by GABA of mutant muscle nAChRs

We next evaluated how mutations at the principal and complementary faces of the binding site that affect ACh-activation also affect activation by GABA.

The amino acid αY190 located at loop C of the principal face of the binding site has

Molecular Pharmacology Fast Forward. Published on December 9, 2014 as DOI: 10.1124/mol.114.095539
This article has not been copyedited and formatted. The final version may differ from this version.

been shown to be essential for muscle (Sine et al., 1994) and α7 (Andersen et al., 2013; Rayes et al., 2009) nAChR activation. The mutation αY190F decreases ACh affinity and the efficacy of activation (Chen et al., 1995; Purohit and Auerbach, 2011; Williams et al., 2011). At the single-channel level, the changes are evidenced by the absence of clusters at high ACh concentrations and briefer opening events (Fig. 2 and Table 1). GABA (1 μM-10 mM) does not elicit detectable single channel activity (n=14) in good agreement with the reduced activation shown for ACh (Table 1).

αG153, located in Loop B of the principal side, is a key residue for ACh activation of mammalian muscle and neuronal α7 nAChRs (Grutter et al., 2003;Jadey et al., 2013). Single-channel kinetic analysis of αG153S nAChR revealed a markedly decreased rate of ACh dissociation, which causes the mutant nAChR to open repeatedly forming bursts (Rayes et al., 2004; Sine et al., 1995) (Fig. 2). In the presence of GABA, kinetic changes are qualitatively similar to those observed in the presence of ACh. Channel openings appear in clear bursts (0.1-500 μM GABA) (Fig. 2). The mean durations of the slowest open component (~1.7 ms, Table 1) and of bursts (4.53 ± 1.69 ms, relative area = 0.26 ± 0.16, n=4) are briefer than those determined in the presence of ACh (~3.7 ms, Table 1) and (10.18 ± 0.35 ms, relative area = 0.61 ± 0.05, n=3) for mean open and burst duration, respectively) ($p<0.01$).

Position 57 of Loop D of the complementary face of the binding site has been shown to be a determinant of drug selectivity (Bartos et al., 2006; Bartos et al., 2009). Recordings from nAChR containing the mutant εG57Q subunit show increased open durations for GABA-activated channels but not for ACh-activated channels with respect to wild-type nAChRs ($p<0.01$, n=3) (Table 1). For receptors carrying the δD57Q mutation, no detectable differences in the mean open duration for both GABA and ACh are observed (Table 1) ($p>0.05$, n=5).

Overall, binding site mutations at the principal face affect similarly GABA and ACh activation whereas position 57 of the ε subunit located at the complementary face

Molecular Pharmacology Fast Forward. Published on December 9, 2014 as DOI: 10.1124/mol.114.095539
This article has not been copyedited and formatted. The final version may differ from this version.

changes GABA but not ACh activation.

To gain more insights into GABA activation, the importance of the α/δ binding-site interface was evaluated by studying activation of nAChR lacking the ε subunit. In the absence of this subunit, nAChRs contain two α/δ binding site interfaces instead of one α/δ and one α/ε interface as in wild-type nAChR. These receptors express well in cells and are activated by ACh (Bouzat et al., 1994). ACh-elicited openings are more prolonged than those of wild-type nAChR (Fig. 3A). The mean duration of the slowest open component for ACh-activated channels is 5.27 ± 1.37 ms (relative area = 0.77 ± 0.13, n=3) instead of ~1 ms for wild-type nAChR. GABA (10 μM) also elicits single-channel currents from $\alpha_2\beta\delta_2$ receptors (Fig. 3A), indicating that this agonist is capable of activating nAChR through the α/δ interface. In agreement with ACh-elicited activity, the duration of the slowest open component (1.60 ± 0.40 ms, relative area = 0.10 ± 0.05, n = 4) is longer than that of wild-type nAChR when GABA is the agonist ($p<0.05$). Although spontaneous activity of $\alpha_2\beta\delta_2$ receptors has been reported (Zhou et al., 1999) we were not able to record clearly detectable openings in this study in the absence of agonist. This difference may be due to differences in receptor expression since the open probability of ligand-free activated receptors is very low. Thus, we can ensure that the detected openings arise from GABA-activated nAChR.

The mutation εT264P at the M2 domain of the ε subunit, which has been first described in a patient suffering from a slow-channel congenital myasthenic syndrome, leads to gain of function (Engel et al., 2012; Ohno et al., 1995). In the absence of ACh, spontaneous activity of the mutant εT264P nAChR is evidenced by the presence of brief openings (Fig. 3B), being the mean duration of the longest duration open component of 1.5 ± 0.3 ms (relative area = 0.05 ± 0.01, n=3). In the presence of ACh (1 μM) or GABA (0.1-100 μM) significantly prolonged openings are observed (Fig. 3B). Open time histograms are fitted by three components, and the slowest one, which is not detected in the absence of agonist, shows a mean duration of 20.62 ± 7.84 ms for 1

Molecular Pharmacology Fast Forward. Published on December 9, 2014 as DOI: 10.1124/mol.114.095539
This article has not been copyedited and formatted. The final version may differ from this version.

μM ACh (relative area = 0.56 ± 0.08, n=3) and 28.45 ± 3.45 ms for 0.1 μM GABA (relative area = 0.81 ± 0.05, n=3). Thus, GABA behaves very similar to ACh in this M2 mutant receptor.

GABA cannot activate α7 nAChR

We evaluated if GABA is able to activate human α7 and the high conductance form of the chimeric α7-5HT$_3$A receptor, which is a good model for studies of α7 since it shows high surface expression and channel activity is easily detected (Andersen et al., 2011; Rayes et al., 2005). In cells transfected with α7 (Fig. 4A) or α7-5HT$_3$A (Fig. 4B) macroscopic currents are elicited by 300 μM ACh (Bouzat et al., 2008). In contrast, application of 1-10 mM GABA to cells showing ACh responses does not generate detectable macroscopic currents (Fig. 4). No single-channel activity from cells expressing α7 (n= 18) or α7-5HT$_3$A receptors (n=20) is detected in the presence of 100-1000 μM GABA. In contrast, typical single-channel openings with mean durations of ~0.28 ms for α7 (100 μM ACh) and ~9.5 ms for α7-5HT$_3$A (500 μM ACh) (Bouzat et al., 2008; Rayes et al., 2005) are detected (Fig. 4A and B). In the α7-5HT$_3$A receptor we tested if a mutation at position 153 of the extracellular domain (α7G153E), which has been shown to increase efficacy in muscle and α7 nAChRs (Bartos et al., 2006; Jadey et al., 2013), allows detectable single-channel activity elicited by GABA..In contrast to the results observed in muscle nAChR, channel activity was not detected in the presence of GABA in α7-5HT$_3$A carrying the G153E mutation (500 and 1000 μM, n=13) (Fig. 4C).

We also explored if the presence of GABA affects α7 activity. To this end, we recorded α7-5HT$_3$A channels in the presence of 300 μM ACh in the tip of the pipette and 300 μM ACh plus 10 mM GABA in the shaft. Under these conditions, competition of GABA should be evidenced as a marked reduction of the frequency of channel openings with time of recording due to the diffusion of GABA to the pipette tip. The

Molecular Pharmacology Fast Forward. Published on December 9, 2014 as DOI: 10.1124/mol.114.095539
This article has not been copyedited and formatted. The final version may differ from this version.

time-dependent decrease in channel activity (67 %), which was measured by the decrease in the number of openings/min between min 1 and 5 of the recording, was not markedly different to that observed for control conditions –only ACh present (61 %)- thus evidencing that GABA does not antagonize ACh-action at α7 receptors.

Docking of GABA into nAChRs

To gain insights into how GABA may interact with nAChRs, we performed *in silico* studies. For the adult muscle nAChR, docking of ACh in both α–ε and α–δ interfaces resulted in only one energetically favorable model, with best binding energy (BBE) of -5.0 kcal/ mol. We observed the well-known cation-π interaction between the positively charged group of ACh and the aromatic ring of αW149 (Dougherty, 2007). ACh also showed the possibility to form a hydrogen bond between its carbonyl group and the polar backbone hydrogen of δL121 or εL119, a hydrogen bond with δ– or ε–Y104, and to interact with W55 at the complementary face (Fig 5A for α/ε).

For GABA, two plausible models were detected for the α–ε interface, named *Model 1* (Fig. 5B) and *Model 2* (Fig. 5C), with BBE of -3.5 and -3.0 kcal/mol, respectively. The probability to adopt one orientation or the other appears to be similar. For the α–δ interface, all docking runs were clustered into only one group with a similar orientation and BBE as that of *Model 1*. *Model 1* is able to reproduce most of the features of ACh interaction (Fig. 5B). The carboxyl group of GABA shows the potential to form an hydrogen bond with Y104 and δL121 or εL119 of the complementary face and the ammonium group shows the potential to form hydrogen bonds with the oxygen of the backbone of αW149 (Hibbs et al., 2009; Xiu et al., 2009). The cation-π interaction with the indole group of W149 is also present. In *Model 2* GABA adopts a different orientation (Fig. 5C). Although the cation-π interaction and the hydrogen bond with W149 is present, its carboxyl group is oriented towards the lower part of the cleft containing aromatic residues, thus avoiding other possible interactions with residues of

Molecular Pharmacology Fast Forward. Published on December 9, 2014 as DOI: 10.1124/mol.114.095539
This article has not been copyedited and formatted. The final version may differ from this version.

Loop E from the complementary face (Supplemental Fig. 1). In *Model 2* orientation, GABA does not occupy the same space as ACh within the binding pocket and it may have the potential to interact with Loop A and to form a hydrogen bond with Y93 (Hansen et al., 2005; Rucktooa et al., 2009).

For each α7-α7 interface, docking of ACh resulted in only one energetically favorable model with BBE of -5.0 kcal/ mol (Fig. 5D). All interactions are similar to those observed for muscle interfaces, with the exception of the hydrogen bond with Y104, which is phenylalanine in α7. In contrast, GABA shows two plausible models, with similar orientations to those in α-ε interface. However, the probability to adopt *Model 2* conformation is two-fold higher than that of *Model 1*. In *Model 1* orientation, it shows the potential to form the cation-π interaction and the hydrogen bond with W149 (Fig. 5E). GABA may also form hydrogen bonds with L119 and with N107, which is not observed in our model of muscle nAChR interfaces. In *Model 2* orientation, the majority of key interactions are similar to those observed in the muscle nAChR (Fig. 5F, Supplemental Fig. 1).

Molecular Pharmacology Fast Forward. Published on December 9, 2014 as DOI: 10.1124/mol.114.095539
This article has not been copyedited and formatted. The final version may differ from this version.

Discussion

We here demonstrate that GABA behaves as a partial agonist of the muscle nAChR but cannot activate the neuronal α7 nAChR.

Macroscopic current recordings show that maximal peak currents of muscle nAChRs elicited by GABA are only 10 % of those elicited by ACh, and dose response curves show that the EC50 is 15-fold higher for GABA than ACh, indicating that GABA is a low-efficacy agonist of the muscle nAChR. At the single-channel level, the mechanistic basis of this weak agonistic efficacy is revealed by: i) the requirement of ~20-fold higher concentration of GABA than ACh (1 μM instead of 50 nM for ACh, (Spitzmaul et al., 2004)) for detectable reliable channel activity; ii) the presence of a major population of brief openings, and, iii) the absence of clusters at all GABA concentrations, in contrast to what is observed with ACh or other agonists (Bouzat et al., 2000).

We explored if GABA requires similar residues to those shown for efficient ACh-activation in the muscle nAChR. We demonstrated that key residues of the principal face, Y190 located in loop C, and G153, located in Loop B, are also required for GABA-activation of muscle nAChR. The effects of αY190F and αG153S mutations on muscle nAChR activation have been well characterized (Grutter et al., 2003; Jadey et al., 2013; Mukhtasimova et al., 2009; Purohit and Auerbach, 2011; Purohit and Auerbach, 2013; Rayes et al., 2004; Salamone et al., 1999; Sine et al., 1995). In parallel with the changes observed for ACh, GABA responses are increased in αG153S mutant and are negligible in αY190F mutant.

Position 153 at Loop B of the binding site has been shown to be associated with a slow-channel syndrome (Sine et al., 1995), to be involved in the high efficacy of activation of nematode nAChRs by anthelmintic drugs (Rayes et al., 2004), to affect gating in neuronal nAChR (Grutter et al., 2003), and to affect agonist efficacy of muscle nAChR (Purohit and Auerbach, 2011). GABA is capable of eliciting bursts of openings,

Molecular Pharmacology Fast Forward. Published on December 9, 2014 as DOI: 10.1124/mol.114.095539
This article has not been copyedited and formatted. The final version may differ from this version.

which are significantly prolonged in the αG153S when compared to the wild-type nAChR. Nevertheless, open and burst durations are briefer than those determined in the presence of ACh. This result indicates that these positions, Y190 and G153 are not determinants of GABA partial agonism but they are important for GABA as well as for ACh activation.

Our study reveals that the residue at position 57 located in Loop D of the complementary face of the α/ε binding site is a key determinant of the action of GABA at muscle nAChR. The mutation εG57Q selectively increases the efficacy of GABA activation, as evidenced by significantly increased open channel durations and by the presence of bursts. As described before (Bartos et al., 2009), ACh-activation is not modified in the mutant εG57Q with respect to the control. The equivalent mutation in the δ subunit does not affect either GABA or ACh activation. These results suggest that GABA binds to the α/ε interface, and that εG57 is involved in its activation. An alternative explanation could be that GABA does not bind to the α-ε interface except in the presence of the εG57Q mutation. Under this hypothesis, the major proportion of brief openings detected in wild-type nAChRs would correspond to openings of single-liganded receptors (α/δ interface). The mutation would lead to more prolonged openings -corresponding to biliganded receptors- by allowing binding of GABA to the α/ε interface. For this to occur, GABA must be able to bind to the α/δ interface. To test this possibility, we studied receptors lacking the ε subunit since unfortunately, it is not possible to detect channel openings from δ-lacking receptors (Bouzat et al., 1994; Zhou et al., 1999). We found that GABA is capable of mediating activation through the α/δ interface. In the presence of GABA, single-channel currents from $\alpha_2\beta\delta_2$ occur in bursts of prolonged openings, which are significantly different to those detected in the absence of agonist, thus indicating that GABA can activate the receptor through the α/δ interface. The mutation εG57Q has been shown to increase significantly the efficacy of morantel activation (Bartos et al., 2009). Thus, the present results reinforce the role of

Molecular Pharmacology Fast Forward. Published on December 9, 2014 as DOI: 10.1124/mol.114.095539
This article has not been copyedited and formatted. The final version may differ from this version.

position 57 as a determinant of selectivity for a broader spectrum of drugs (Bartos et al., 2006; Shimomura et al., 2002).

Docking studies showed only one possible way of interaction of ACh and of GABA at the α/δ interface but two of GABA at α/ε and α7/α7 interfaces. *Models 1* and *2* differ in the orientation of the GABA molecule, which can form the H-bonds and cation-π interactions with key residues of the binding site (Y93, W149 of the principal face and Y104, N107 or L119/L121 of the complementary face), similar to those observed for ACh and other agonists. In the light of these observations, the partial agonism of GABA at muscle nAChRs may be explained by its ability of adopting multiple orientations at the binding site, as reported previously for other partial agonists (Hibbs et al., 2009). Considering our experimental evidence that GABA can activate nAChR through the α/δ subunit interface, we can suggest that *Model 1* corresponds to the most probable orientation associated with activation. The apparent controversy between our experimental results, which reveal lack of functional interaction of GABA with α7, and our docking results, which show GABA orientations at α7/α7 similar to those at α/ε, may have different explanations. A possible explanation is related to the prevalence of *Model 2* orientation in α7, in which GABA does not occupy the same space as ACh within the binding pocket, and it may therefore neither be able to elicit receptor activation nor to compete with ACh. It could be also possible that although the overall orientations of GABA appear similar in α/ε and α7/α7 interfaces, differences in specific potential interactions may be involved in the differential selectivity. Also, Loop F, which could not be included in our homology models, may be involved in the differential actions of GABA since it has been shown to be a determinant for drug selectivity and partial agonism (Stokes et al., 2004; Hibbs et al. 2009). Alternatively, other residues located outside the binding site but involved in coupling agonist binding to channel opening may influence the capability of GABA to activate muscle but not α7 nAChRs. Although conclusions from our docking results should be considered with caution, they

Molecular Pharmacology Fast Forward. Published on December 9, 2014 as DOI: 10.1124/mol.114.095539
This article has not been copyedited and formatted. The final version may differ from this version.

open doors for further research.

Plasma GABA concentration in healthy individuals is around 0.1 μM (Bjork et al., 2001). It has been proposed that peripheral lymphocytes, which have a complete GABAergic system (Dionisio et al., 2011), could be a source of plasmatic GABA. The lack of α7 activation by GABA is therefore important since this receptor is present in blood cells (De Rosa et al., 2009;Wessler and Kirkpatrick, 2008) and it is therefore continuously exposed to serum GABA. Even at higher GABA concentrations, α7 cannot be activated by GABA, which is also important to avoid crosstalk at the synaptic level by spillover of GABA, which may diffuse locally (Fabian-Fine et al., 2001;Zago et al., 2006). It would be interesting to explore if other neuronal nAChRs, such as α4β2, can be activated by GABA.

Serum GABA concentration is not high enough to activate muscle nAChRs. However, we found that mutant muscle nAChRs associated with slow-channel congenital myasthenic syndromes (αG153S and εT264P mutants) are activated by 0.1 μM GABA, a concentration reached in plasma. For both gain-of-function receptors, single-channel activity in the presence of GABA is significantly different from that observed in the absence of neurotransmitter. Moreover, the mean duration of both bursts and openings is similar for ACh- and GABA-activated εT264P nAChRs. Thus, slow-channel congenital myasthenic syndrome nAChRs at the neuromuscular junction are likely to be activated by steady exposure to serum GABA. This continuous channel activity may contribute to the pathophysiology of the disease. Interestingly, a similar effect has been proposed for serum choline at nAChR from slow-channel congenital syndromes (Zhou et al., 1999).

In conclusion, GABA cannot activate neuronal α7 receptors, a feature extremely important for preserving an adequate excitatory/inhibitory balance. On the other hand, muscle nAChRs are partially activated by GABA and mutations at the principal face of the binding site affect GABA-activation in the same manner as ACh-activation. This

Molecular Pharmacology Fast Forward. Published on December 9, 2014 as DOI: 10.1124/mol.114.095539
This article has not been copyedited and formatted. The final version may differ from this version.

activity elicited by GABA could be important in the progression of congenital myasthenic syndromes associated to gain-of-function mutations.

Molecular Pharmacology Fast Forward. Published on December 9, 2014 as DOI: 10.1124/mol.114.095539
This article has not been copyedited and formatted. The final version may differ from this version.

Author Contribution

Participated in research design: Dionisio, Bergé, Bouzat.

Conducted experiments: Dionisio, Bergé, Bravo, Bouzat

Performed data analysis: Dionisio, Bergé, Bravo, Esandi, Bouzat

Wrote or contributed to the writing of the manuscript: Dionisio, Bergé, Esandi, Bouzat

References

Andersen N, Corradi J, Bartos M, Sine S M and Bouzat C (2011) Functional Relationships Between Agonist Binding Sites and Coupling Regions of Homomeric Cys-Loop Receptors. J Neurosci 31:3662-3669.

Andersen N, Corradi J, Sine S M and Bouzat C (2013) Stoichiometry for Activation of Neuronal Alpha7 Nicotinic Receptors. Proc Natl Acad Sci U S A 110:20819-20824.

Andersson U and Tracey K J (2012) Reflex Principles of Immunological Homeostasis. Annu Rev Immunol 30:313-335.

Arias HR, De Rosa M J, Berge I, Feuerbach D and Bouzat C (2013) Differential Pharmacological Activity of JN403 Between Alpha7 and Muscle Nicotinic Acetylcholine Receptors. Biochemistry 52:8480-8488.

Bartos M, Corradi J and Bouzat C (2009) Structural Basis of Activation of Cys-Loop Receptors: the Extracellular-Transmembrane Interface As a Coupling Region. Mol Neurobiol 40:236-252.

Bartos M, Rayes D and Bouzat C (2006) Molecular Determinants of Pyrantel Selectivity in Nicotinic Receptors. Mol Pharmacol 70:1307-1318.

Bjork JM, Moeller F G, Kramer G L, Kram M, Suris A, Rush A J and Petty F (2001) Plasma GABA Levels Correlate With Aggressiveness in Relatives of Patients With Unipolar Depressive Disorder. Psychiatry Res 101:131-136.

Bouzat C (2012) New Insights into the Structural Bases of Activation of Cys-Loop

Receptors. J Physiol Paris 106:23-33.

Bouzat C, Barrantes F and Sine S (2000) Nicotinic Receptor Fourth Transmembrane Domain: Hydrogen Bonding by Conserved Threonine Contributes to Channel Gating Kinetics. J Gen Physiol 115:663-672.

Bouzat C, Bartos M, Corradi J and Sine S M (2008) The Interface Between Extracellular and Transmembrane Domains of Homomeric Cys-Loop Receptors Governs Open-Channel Lifetime and Rate of Desensitization. J Neurosci 28:7808-7819.

Bouzat C, Bren N and Sine S M (1994) Structural Basis of the Different Gating Kinetics of Fetal and Adult Acetylcholine Receptors. Neuron 13:1395-1402.

Bouzat C, Gumilar F, del Carmen E M and Sine S M (2002) Subunit-Selective Contribution to Channel Gating of the M4 Domain of the Nicotinic Receptor. Biophys J 82:1920-1929.

Bouzat C, Gumilar F, Spitzmaul G, Wang H L, Rayes D, Hansen S B, Taylor P and Sine S M (2004) Coupling of Agonist Binding to Channel Gating in an ACh-Binding Protein Linked to an Ion Channel. Nature 430:896-900.

Brejc K, van Dijk W J, Klaassen R V, Schuurmans M, van Der O J, Smit A B and Sixma T K (2001) Crystal Structure of an ACh-Binding Protein Reveals the Ligand-Binding Domain of Nicotinic Receptors. Nature 411:269-276.

Chen Q, Fletcher G H and Steinbach J H (1995) Selection of Stably Transfected Cells Expressing a High Level of Fetal Muscle Nicotinic Receptors. J Neurosci Res 40:606-

612.

Corradi J, Gumilar F and Bouzat C (2009) Single-Channel Kinetic Analysis for Activation and Desensitization of Homomeric 5-HT(3)A Receptors. Biophys J 97:1335-1345.

De Rosa MJ, Dionisio L, Agriello E, Bouzat C and Esandi M C (2009) Alpha 7 Nicotinic Acetylcholine Receptor Modulates Lymphocyte Activation. Life Sci 85:444-449.

Dionisio L, Jose De R M, Bouzat C and Esandi M C (2011) An Intrinsic GABAergic System in Human Lymphocytes. Neuropharmacology 60:513-519.

Dougherty DA (2007) Cation-Pi Interactions Involving Aromatic Amino Acids. J Nutr 137:1504S-1508S.

Engel AG, Shen X M, Selcen D and Sine S (2012) New Horizons for Congenital Myasthenic Syndromes. Ann N Y Acad Sci 1275:54-62.

Fabian-Fine R, Skehel P, Errington M L, Davies H A, Sher E, Stewart M G and Fine A (2001) Ultrastructural Distribution of the Alpha7 Nicotinic Acetylcholine Receptor Subunit in Rat Hippocampus. J Neurosci 21:7993-8003.

Grutter T, Prado de C L, Le N N, Corringer P J, Edelstein S and Changeux J P (2003) An H-Bond Between Two Residues From Different Loops of the Acetylcholine Binding Site Contributes to the Activation Mechanism of Nicotinic Receptors. EMBO J 22:1990-2003.

Hamill OP, Marty A, Neher E, Sakmann B and Sigworth F J (1981) Improved Patch-

Clamp Techniques for High-Resolution Current Recording From Cells and Cell-Free Membrane Patches. Pflugers Arch 391:85-100.

Hansen SB, Sulzenbacher G, Huxford T, Marchot P, Taylor P and Bourne Y (2005) Structures of Aplysia AChBP Complexes With Nicotinic Agonists and Antagonists Reveal Distinctive Binding Interfaces and Conformations. EMBO J 24:3635-3646.

Hernando G, Berge I, Rayes D and Bouzat C (2012) Contribution of Subunits to Caenorhabditis Elegans Levamisole-Sensitive Nicotinic Receptor Function. Mol Pharmacol 82:550-560.

Hibbs RE, Sulzenbacher G, Shi J, Talley T T, Conrod S, Kem W R, Taylor P, Marchot P and Bourne Y (2009) Structural Determinants for Interaction of Partial Agonists With Acetylcholine Binding Protein and Neuronal Alpha7 Nicotinic Acetylcholine Receptor. EMBO J 28:3040-3051.

Hurst R, Rollema H and Bertrand D (2013) Nicotinic Acetylcholine Receptors: From Basic Science to Therapeutics. Pharmacol Ther 137:22-54.

Jadey S, Purohit P and Auerbach A (2013) Action of Nicotine and Analogs on Acetylcholine Receptors Having Mutations of Transmitter-Binding Site Residue AlphaG153. J Gen Physiol 141:95-104.

Kalamida D, Poulas K, Avramopoulou V, Fostieri E, Lagoumintzis G, Lazaridis K, Sideri A, Zouridakis M and Tzartos S J (2007) Muscle and Neuronal Nicotinic Acetylcholine Receptors. Structure, Function and Pathogenicity. FEBS J 274:3799-3845.

Kullmann DM, Ruiz A, Rusakov D M, Scott R, Semyanov A and Walker M C (2005)

Presynaptic, Extrasynaptic and Axonal GABAA Receptors in the CNS: Where and Why? Prog Biophys Mol Biol 87:33-46.

Lendvai B and Vizi E S (2008) Nonsynaptic Chemical Transmission Through Nicotinic Acetylcholine Receptors. Physiol Rev 88:333-349.

Matsuda K, Shimomura M, Ihara M, Akamatsu M and Sattelle D B (2005) Neonicotinoids Show Selective and Diverse Actions on Their Nicotinic Receptor Targets: Electrophysiology, Molecular Biology, and Receptor Modeling Studies. Biosci Biotechnol Biochem 69:1442-1452.

McCann CM, Bracamontes J, Steinbach JH and Sanes JR. (2006) The cholinergic antagonist alpha-bungarotoxin also binds and blocks a subset of GABA receptors. PNAS 103:5149-5154.

Morris GM, Huey R, Lindstrom W, Sanner M F, Belew R K, Goodsell D S and Olson A J (2009) AutoDock4 and AutoDockTools4: Automated Docking With Selective Receptor Flexibility. J Comput Chem 30:2785-2791.

Mukhtasimova N, Lee W Y, Wang H L and Sine S M (2009) Detection and Trapping of Intermediate States Priming Nicotinic Receptor Channel Opening. Nature 459:451-454.

Nys M, Kesters D and Ulens C (2013) Structural Insights into Cys-Loop Receptor Function and Ligand Recognition. Biochem Pharmacol 86:1042-1053.

Ohno K, Hutchinson D O, Milone M, Brengman J M, Bouzat C, Sine S M and Engel A G (1995) Congenital Myasthenic Syndrome Caused by Prolonged Acetylcholine Receptor Channel Openings Due to a Mutation in the M2 Domain of the Epsilon Subunit. Proc

Natl Acad Sci U S A 92:758-762.

Olah S, Fule M, Komlosi G, Varga C, Baldi R, Barzo P and Tamas G (2009) Regulation of Cortical Microcircuits by Unitary GABA-Mediated Volume Transmission. Nature 461:1278-1281.

Pear WS, Nolan GP, Scott ML and Baltimore D. (1993) Production of high-titer helper - free retroviruses by transient transfection. PNAS 90: 8392-8396.

Purohit P and Auerbach A (2011) Glycine Hinges With Opposing Actions at the Acetylcholine Receptor-Channel Transmitter Binding Site. Mol Pharmacol 79:351-359.

Purohit P and Auerbach A (2013) Loop C and the Mechanism of Acetylcholine Receptor-Channel Gating. J Gen Physiol 141:467-478.

Rayes D, De Rosa M J, Bartos M and Bouzat C (2004) Molecular Basis of the Differential Sensitivity of Nematode and Mammalian Muscle to the Anthelmintic Agent Levamisole. J Biol Chem 279:36372-36381.

Rayes D, De Rosa M J, Sine S M and Bouzat C (2009) Number and Locations of Agonist Binding Sites Required to Activate Homomeric Cys-Loop Receptors. J Neurosci 29:6022-6032.

Rayes D, Spitzmaul G, Sine S M and Bouzat C (2005) Single-Channel Kinetic Analysis of Chimeric Alpha7-5HT3A Receptors. Mol Pharmacol 68:1475-1483.

Rucktooa P, Smit A B and Sixma T K (2009) Insight in NAChR Subtype Selectivity From AChBP Crystal Structures. Biochem Pharmacol 78:777-787.

Salamone FN, Zhou M and Auerbach A (1999) A Re-Examination of Adult Mouse Nicotinic Acetylcholine Receptor Channel Activation Kinetics. J Physiol 516 (Pt 2):315-330.

Sali A, Potterton L, Yuan F, van V H and Karplus M (1995) Evaluation of Comparative Protein Modeling by MODELLER. Proteins 23:318-326.

Shimomura M, Okuda H, Matsuda K, Komai K, Akamatsu M and Sattelle D B (2002) Effects of Mutations of a Glutamine Residue in Loop D of the Alpha7 Nicotinic Acetylcholine Receptor on Agonist Profiles for Neonicotinoid Insecticides and Related Ligands. Br J Pharmacol 137:162-169.

Sine SM and Engel A G (2006) Recent Advances in Cys-Loop Receptor Structure and Function. Nature 440:448-455.

Sine SM, Ohno K, Bouzat C, Auerbach A, Milone M, Pruitt J N and Engel A G (1995) Mutation of the Acetylcholine Receptor Alpha Subunit Causes a Slow-Channel Myasthenic Syndrome by Enhancing Agonist Binding Affinity. Neuron 15:229-239.

Sine SM, Quiram P, Papanikolaou F, Kreienkamp H J and Taylor P (1994) Conserved Tyrosines in the Alpha Subunit of the Nicotinic Acetylcholine Receptor Stabilize Quaternary Ammonium Groups of Agonists and Curariform Antagonists. J Biol Chem 269:8808-8816.

Sine SM, Shen X M, Wang H L, Ohno K, Lee W Y, Tsujino A, Brengmann J, Bren N, Vajsar J and Engel A G (2002) Naturally Occurring Mutations at the Acetylcholine Receptor Binding Site Independently Alter ACh Binding and Channel Gating. J Gen Physiol 120:483-496.

Spitzmaul G, Corradi J and Bouzat C (2004) Mechanistic Contributions of Residues in the M1 Transmembrane Domain of the Nicotinic Receptor to Channel Gating. Mol Membr Biol 21:39-50.

Stokes C, Porter Papke J K, Horenstein N A, Kem W R, McCormack T J and Papke R L (2004) The structural basis for GTS-21 selectivity between human and rat nicotinic α7 receptors. Mol Pharmacol 66:14–24.

Thomsen MS, Hansen H H, Timmerman D B and Mikkelsen J D (2010) Cognitive Improvement by Activation of Alpha7 Nicotinic Acetylcholine Receptors: From Animal Models to Human Pathophysiology. Curr Pharm Des 16:323-343.

Wallace TL and Bertrand D (2013) Alpha7 Neuronal Nicotinic Receptors As a Drug Target in Schizophrenia. Expert Opin Ther Targets 17:139-155.

Wallace TL and Porter R H (2011) Targeting the Nicotinic Alpha7 Acetylcholine Receptor to Enhance Cognition in Disease. Biochem Pharmacol 82:891-903.

Wessler I and Kirkpatrick C J (2008) Acetylcholine Beyond Neurons: the Non-Neuronal Cholinergic System in Humans. Br J Pharmacol 154:1558-1571.

Williams DK, Stokes C, Horenstein N A and Papke R L (2011) The Effective Opening of Nicotinic Acetylcholine Receptors With Single Agonist Binding Sites. J Gen Physiol 137:369-384.

Williams ME, Burton B, Urrutia A, Shcherbatko A, Chavez-Noriega L E, Cohen C J and Aiyar J (2005) Ric-3 Promotes Functional Expression of the Nicotinic Acetylcholine Receptor Alpha7 Subunit in Mammalian Cells. J Biol Chem 280:1257-1263.

Xiu X, Puskar N L, Shanata J A, Lester H A and Dougherty D A (2009) Nicotine Binding to Brain Receptors Requires a Strong Cation-Pi Interaction. Nature 458:534-537.

Zago WM, Massey K A and Berg D K (2006) Nicotinic Activity Stabilizes Convergence of Nicotinic and GABAergic Synapses on Filopodia of Hippocampal Interneurons. Mol Cell Neurosci 31:549-559.

Zhou M, Engel A G and Auerbach A (1999) Serum Choline Activates Mutant Acetylcholine Receptors That Cause Slow Channel Congenital Myasthenic Syndromes. Proc Natl Acad Sci U S A 96:10466-10471.

Molecular Pharmacology Fast Forward. Published on December 9, 2014 as DOI: 10.1124/mol.114.095539
This article has not been copyedited and formatted. The final version may differ from this version.

Footnotes

a) **Dionisio L.** and **Bergé I.** contributed equally to the work.

b) **Financial Support:** Supported by Universidad Nacional del Sur (UNS), Agencia Nacional de Promoción Científica y Tecnológica (ANPCYT), and Consejo Nacional de Investigaciones Científicas y Técnicas (CONICET).

c) **This study has been presented in 39**th annual meeting of Argentinean Biophysycal Society, Workshop CeBEM and Latin American Protein Society Meeting. Salta, Argentina. October 2010 Poster P032. **Bravo M., Dionisio L. and Bouzat C.** “Activation of nicotinic receptors by the neurotransmitter GABA”.

d) **Corresponding author:** Cecilia Bouzat. Instituto de Investigaciones Bioquímicas de Bahía Blanca. Camino La Carrindanga Km 7. 8000 Bahía Blanca. Argentina. E-mail: inbouzat@criba.edu.ar. Telephone: 54-291-4861201-FAX: 54-291-4861200

Molecular Pharmacology Fast Forward. Published on December 9, 2014 as DOI: 10.1124/mol.114.095539
This article has not been copyedited and formatted. The final version may differ from this version.

Figure legends

Figure 1.

Activation of adult muscle nAChR by GABA. A *Left,* whole-cell currents recorded in response to rapid perfusion of 500 µM ACh or 500 µM GABA. The solid bar indicates the duration of exposure to the drug. Each curve is the average of two to four drug applications. *Right,* Dose-response curves for ACh (open symbols) and GABA (solid symbols) of muscle nAChR. Each point is the average of 3-5 determinations, with the error bars representing the S.D. of the mean value. Curves are fits to the Hill equation. Membrane potential -70 mV. **B** Single channels activated by 1 and 1000 µM GABA and 1 and 60 µM ACh recorded from cells expressing adult muscle nAChR. *Left*, traces of currents are shown at a bandwidth of 10 kHz with channel openings as upward deflections. *Right*, open and closed time histograms corresponding to each condition. Membrane potential: -70 mV. **C** Single channel recordings activated by 1000 µM GABA and 1 µM α-BTX were recorded from cells expressing adult muscle nAChR. The tip of the pipette was filled with a solution containing only GABA, and the shaft with the solution containing GABA and α-BTX. After the first minute of recording, a marked decrease of channel activity was observed. Traces are shown at a bandwidth of 7 kHz with channel openings as upward deflections. The inset shows an opening event at higher time resolution. Membrane potential: -70 mV.

Figure 2

Activation of mutant muscle nAChRs by GABA. *Left*, channels were recorded from BOSC 23 cells expressing nAChR containing the mutant αY190F, αG153S, εG57Q or δD57Q subunits. Currents are shown at a bandwidth of 7 kHz with channel openings as upward deflections. *Right*, open and closed time histograms of nAChRs carrying the specified mutant subunit. The data are representative of 4–6 recordings for each

Molecular Pharmacology Fast Forward. Published on December 9, 2014 as DOI: 10.1124/mol.114.095539
This article has not been copyedited and formatted. The final version may differ from this version.

condition. Membrane potential: -70 mV.

Figure 3

A. Activation of triplet $\alpha_2\beta\delta_2$ nAChRs. Single channels activated by 1 µM ACh and 10 µM GABA were recorded from cells expressing adult muscle nAChR lacking the ε subunit. *Left*, traces of currents are shown at a bandwidth of 7 kHz with channel openings as upward deflections. *Right*, open and closed time histograms corresponding to each condition. The data are representative of 4 recordings for each condition. Membrane potential: -70 mV**. B. Activation of εT264P mutant nAChR**. Single channels were recorded from cells expressing adult muscle nAChR carrying the εT264P mutation on the M2 domain in the absence of agonist, and in the presence 1 µM ACh or 0.1 µM GABA. *Left*, traces of currents are shown at a bandwidth of 7 kHz with channel openings as upward deflections. *Right*, open and closed time histograms corresponding to each condition. The data are representative of 5 recordings for each condition. Membrane potential, -70 mV.

Figure 4

Action of GABA on α7 nAChR. A and **B**. *Left,* macroscopic current recordings activated by 1000 µM GABA (grey line) or 300 µM ACh (black line) from cells expressing α7 (A) or α7-5HT$_3$A receptors (B). The solid line above the traces represents the pulse duration of the agonist. Each trace is representative of 4 recordings for each condition. Membrane potential: -70 mV. *Right,* Single-channel traces from cells expressing α7 (A) or α7-5HT$_3$A receptors (B). Traces of currents are shown at a bandwidth of 7 kHz with channel openings as upward deflections. The data are representative of 10 or 20 recordings for each condition. Membrane potential: -70 mV. **C.** Single-channel traces corresponding to α7-5HT$_3$A receptors carrying the α7G153E mutation activated by 500 µM ACh or 1000 µM GABA (no channels detected,

Molecular Pharmacology Fast Forward. Published on December 9, 2014 as DOI: 10.1124/mol.114.095539
This article has not been copyedited and formatted. The final version may differ from this version.

n=13). Openings are shown as upward deflections at a bandwidth of 9 kHz. Membrane potential: -70 mV.

Figure 5

Molecular docking of ACh or GABA to muscle α/ε (Top) or α7/α7 (bottom) interfaces. Homology models of α/ε (A-C) (Data supplement pdb alpha-epsilon interface) and α7/α7 interfaces (D-F) (Data supplement pdb alpha7-alpha7 interface) were generated using the structure of the AChBP (PDB entry 1UW6) as described in Experimental Procedures. The subunits are colored cyan (α), red (ε) and pink (α7), and the corresponding residues atoms are colored as follows: grey for C, violet for N, red for O and light gray for H. ACh and GABA carbons are colored green. The labeled residues are conserved among interfaces except F103 in the α7 subunit of the complementary face, which corresponds to Y104 in the ε subunit. The interactions of ligands with important residues of the binding site are also shown. Hydrogen bonds are shown with black dashed lines and cation-π interactions, with solid lines.

Molecular docking of ACh and GABA to muscle α/ε interface. Pdb alpha-epsilon interface.

Molecular docking of ACh and GABA to α7/α7 interface. Pdb alpha7-alpha7 interface

Molecular Pharmacology Fast Forward. Published on December 9, 2014 as DOI: 10.1124/mol.114.095539
This article has not been copyedited and formatted. The final version may differ from this version.

Table 1. Open durations of wild-type and mutant muscle nAChR activated by ACh and GABA.

Receptor	Agonist	[μM]	Open 1 (ms) (relative area)	Open 2 (ms) (relative area)
wild-type	ACh	1	0.99 ± 0.10 (0.70 ± 0.12)	0.24 ± 0.07 (0.30 ± 0.13)
	GABA	1	0.76 ± 0.12 (0.31 ± 0.04)	0.10 ± 0.03 (0.69 ± 0.04)
αY190F	ACh	60	0.58 ± 0.17 (0.11 ± 0.06)	0.19 ± 0.05 (0.89 ± 0.06)
	GABA	1-10000	nd	
αG153S	ACh	1	3.76 ± 0.29 (0.67 ± 0.07)	0.36 ± 0.04 (0.32 ± 0.07)
	GABA	1	1.68 ± 0.40 (0.39 ± 0.157)	0.18 ± 0.02 (0.60 ± 0.157)
εG57Q	ACh	1	0.88 ± 0.0 (0.18 ± 0,12)	0.32 ± 0.03 (0.82 ± 0,12)
	GABA	1000	1.91 ± 0.33 (0.11 ± 0.01)	0.24 ± 0.03 (0.89 ± 0.01)
δD57Q	ACh	1	1.18 ± 0.25 (0.67 ± 0.08)	0.32 ± 0.06 (0.33 ± 0.08)
	GABA	1000	1.55 ± 0.59 (0.06 ± 0.02)	0.16 ± 0.02 (0.93 ± 0.01)

Single-channel recordings were performed from cells expressing muscle wild-type receptors or receptors containing the indicated mutant subunit. Open duration components were obtained from the open time histograms. Data are shown as mean ± SD for at least 3 recordings for each condition. nd: For αY190F, single-channel activity in the presence of GABA was not detected in 14 different patches from GFP transfected cells (green cells).

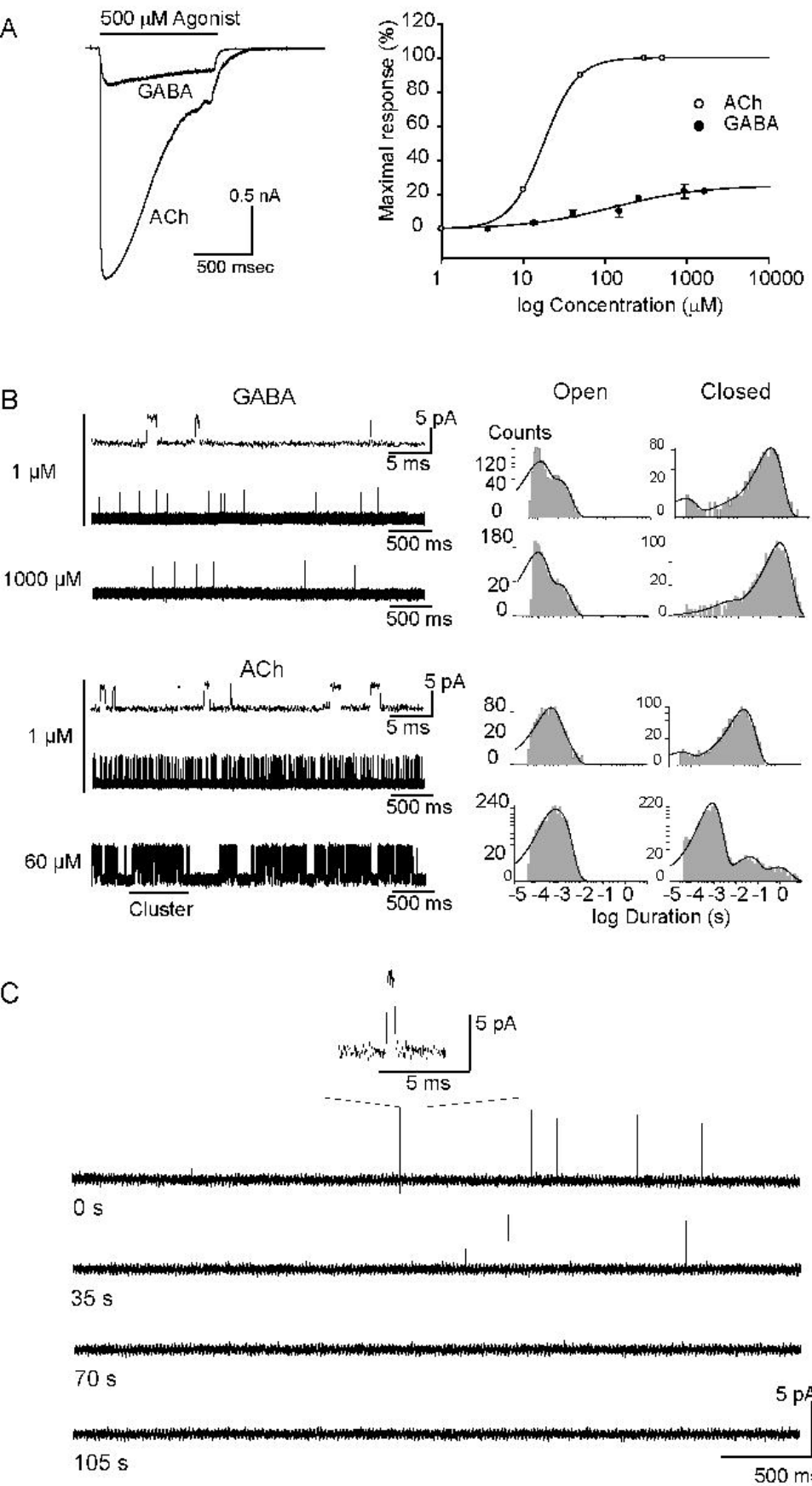
A
500 µM Agonist
GABA
ACh
0.5 nA
500 msec
Maximal response (%)
120
100
80
60
40
20
0
ACh
GABA
1
10
100
1000
10000
log Concentration (µM)
B
GABA
Open
Closed
5 pA
5 ms
1 µM
500 ms
1000 µM
Counts
120
40
0
80
20
180
100
ACh
1 µM
60 µM
Cluster
240
220
-5 -4 -3 -2 -1 0
log Duration (s)
C
5 pA
5 ms
0 s
35 s
70 s
105 s
500 ms

Figure 2

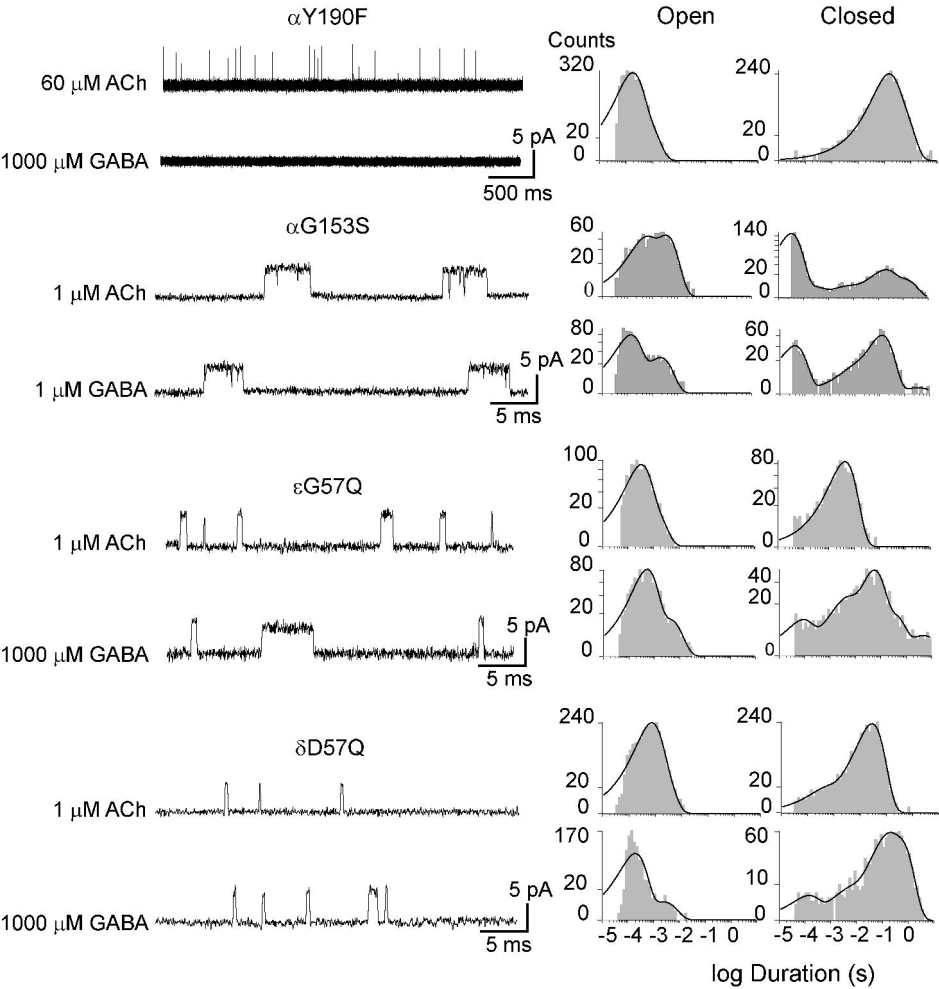
αY190F
Open
Closed
Counts
60 μM ACh
1000 μM GABA
5 pA
500 ms
320
20
0
240
20
0
αG153S
1 μM ACh
1 μM GABA
5 pA
5 ms
60
20
0
140
20
0
80
20
0
60
20
0
εG57Q
1 μM ACh
1000 μM GABA
5 pA
5 ms
100
20
0
80
20
0
80
20
0
40
20
0
δD57Q
1 μM ACh
1000 μM GABA
5 pA
5 ms
240
20
0
240
20
0
170
20
0
60
10
0
-5 -4 -3 -2 -1 0
-5 -4 -3 -2 -1 0
log Duration (s)

Figure 3

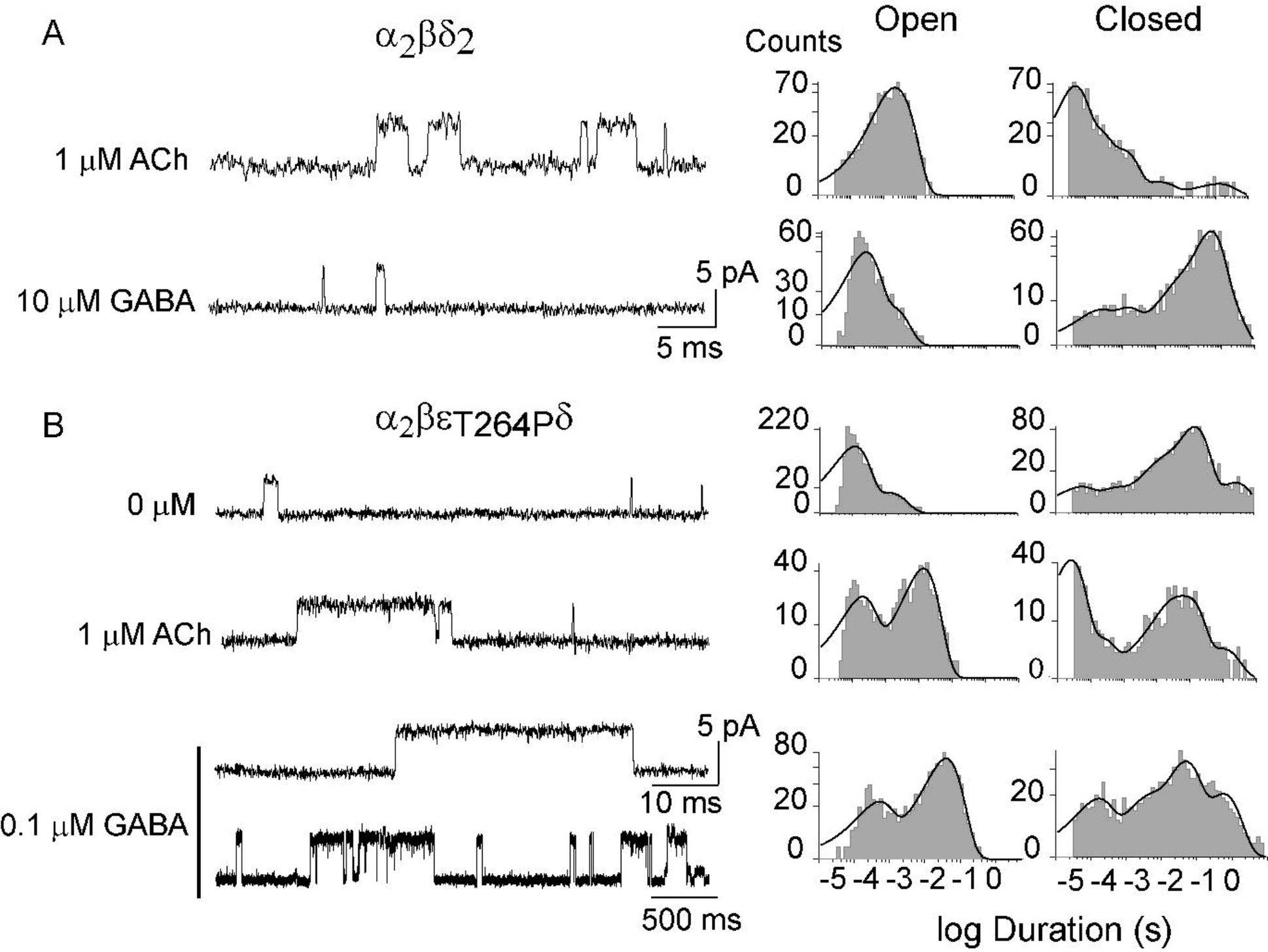
A
$\alpha_2\beta\delta_2$
Open
Closed
Counts
1 μM ACh
10 μM GABA
5 pA
5 ms
70
20
0
60
30
10
B
$\alpha_2\beta\varepsilon T264P\delta$
220
80
40
0 μM
1 μM ACh
0.1 μM GABA
10 ms
500 ms
-5 -4 -3 -2 -1 0
log Duration (s)

Figure 4

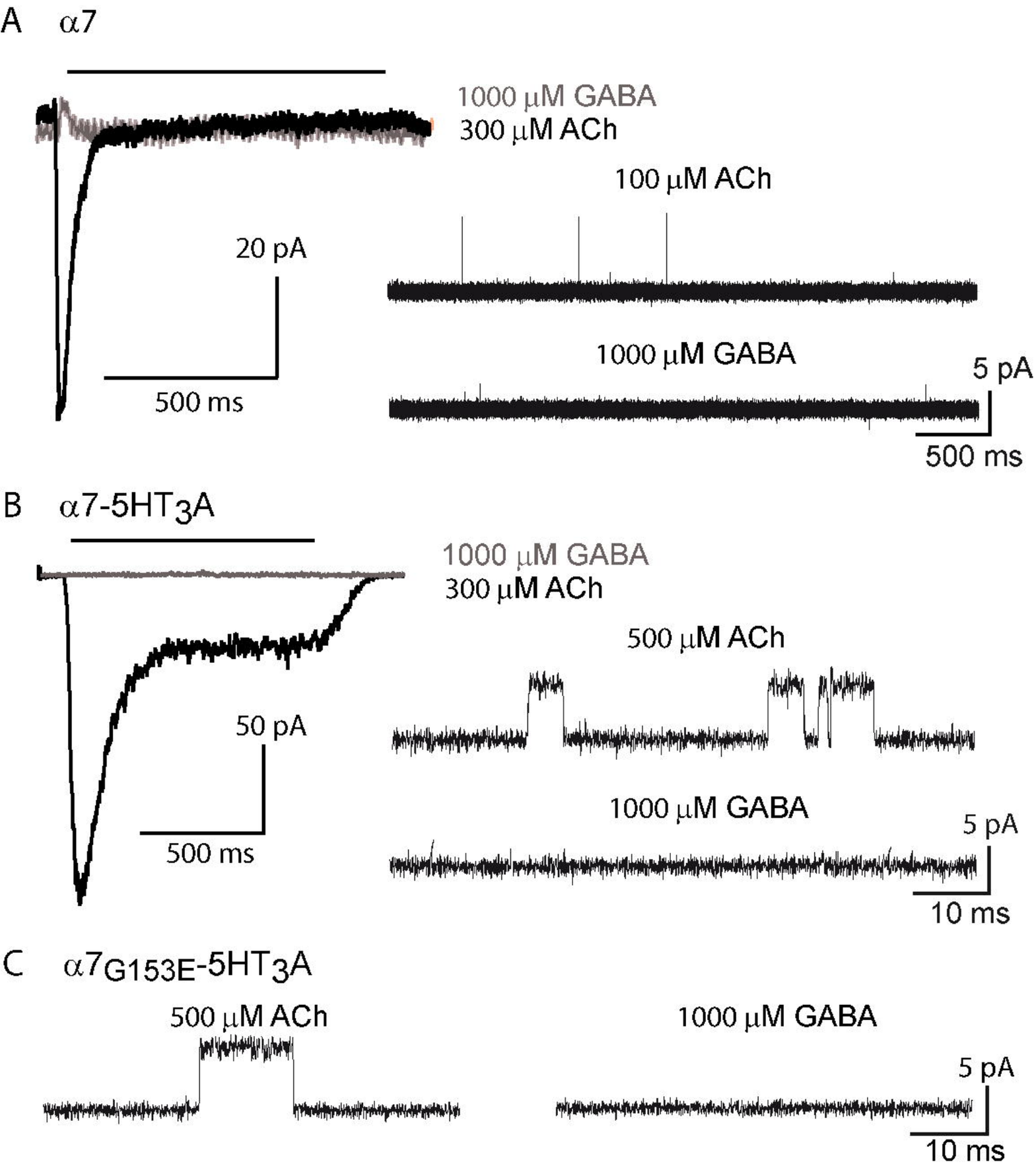
A α7
1000 μM GABA
300 μM ACh
20 pA
500 ms
100 μM ACh
1000 μM GABA
5 pA
500 ms
B α7-5HT3A
1000 μM GABA
300 μM ACh
50 pA
500 ms
500 μM ACh
1000 μM GABA
5 pA
10 ms
C α7G153E-5HT3A
500 μM ACh
1000 μM GABA
5 pA
10 ms

Figure 5

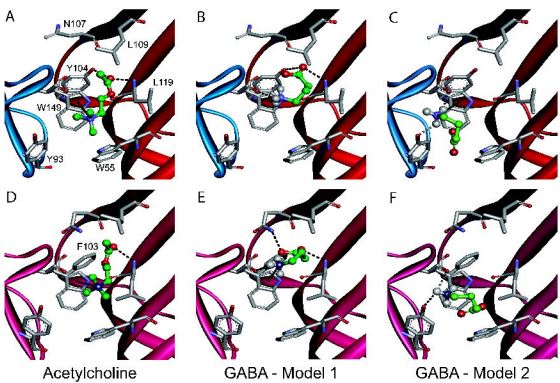
A
B
C
D
E
F
N107
L109
Y104
L119
W149
Y93
W55
F103
α/ε
α7/α7
Acetylcholine
GABA - Model 1
GABA - Model 2

Neurotransmitter GABA activates muscle but not α7 nicotinic receptors

Leonardo Dionisio, Ignacio Bergé, Matías Bravo, María del Carmen Esandi and Cecilia Bouzat

Instituto de Investigaciones Bioquímicas de Bahía Blanca, UNS-CONICET, Camino La Carrindanga Km7, 8000 Bahía Blanca, Argentina.

MOLECULAR PHARMACOLOGY

Supplemental Table 1. *Single-channel properties of muscle nAChR activated at a range of GABA concentration*.

nAChR	[GABA] μM	Open 1 (ms) (relative area)	Open 2 (ms) (relative area)
Muscle Wild-Type	1	0.76 ± 0.12 (0.31 ± 0.04)	0.10 ± 0.03 (0.69 ± 0.04)
	50	0.93 ± 0.25 (0.34 ± 0.10)	0.12 ± 0.09 (0.66 ± 0.10)
	100	1.04 ± 0.30 (0.34 ± 0.23)	0.12 ± 0.04 (0.66 ± 0.23)
	500	0.79 ± 0.10 (0.12 ± 0.08)	0.09 ± 0.01 (0.88 ± 0.08)
	1000	1.07 ± 0.18 (0.17 ± 0.12)	0.08 ± 0.03 (0.83 ± 0.13)
	10000	1.17± 0.28 (0.08 ± 0.10)	0.11 ± 0.03 (0.92 ± 0.10)

Single-channel recordings were performed from cells expressing muscle wild-type nAChRs. Open duration components were obtained from the open time histograms. Data are shown as mean ± SD for at least 3 recordings for each condition.

Supplemental Figure 1

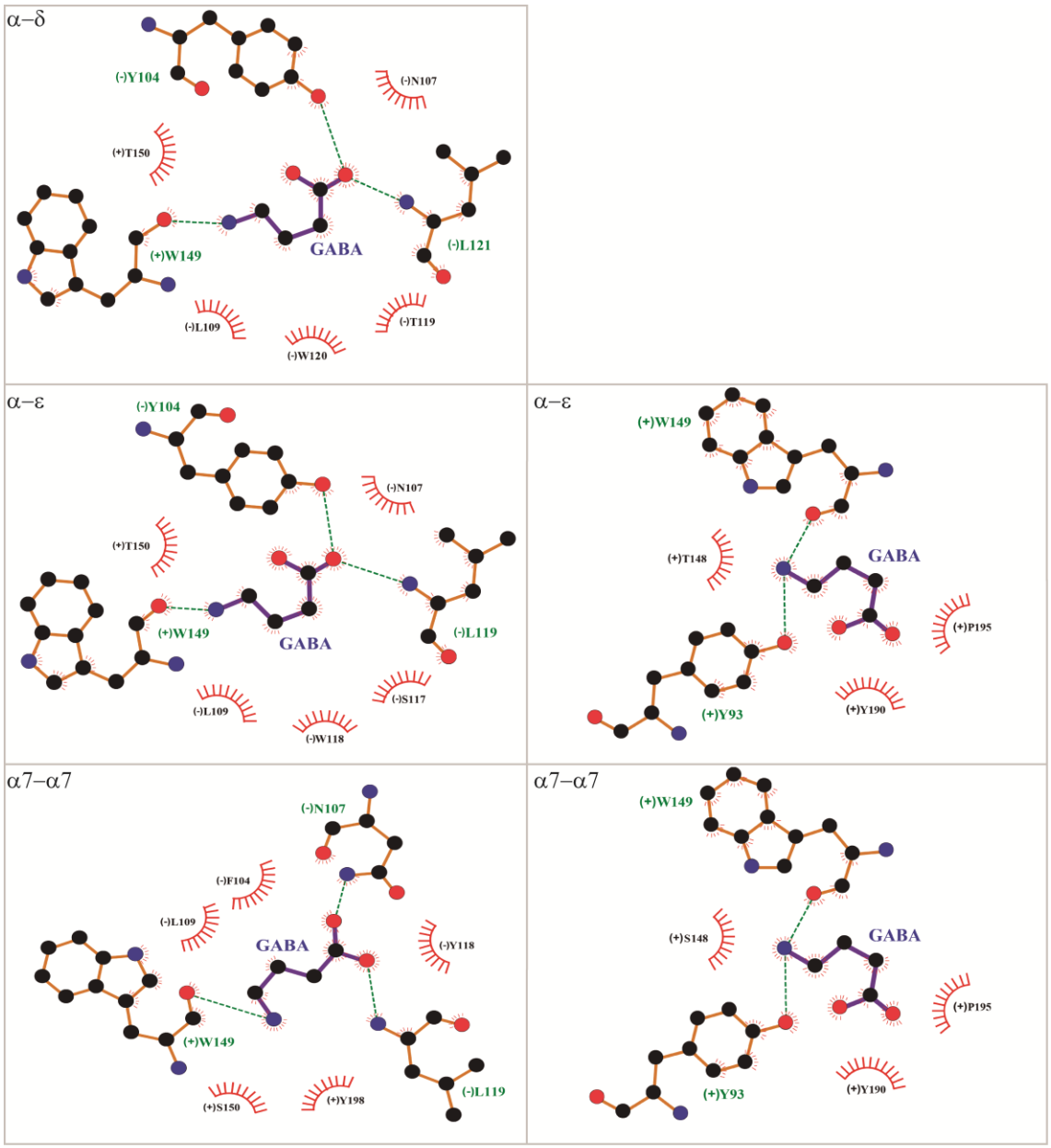

GABA - Model 1 GABA - Model 2

Ligplot diagrams illustrating protein-ligand interactions during docking. Ligand is shown in violet and the corresponding ligand and amino acid atoms are colored as follows: black for C, red for O and blue for N. Hydrogen bonds are shown as green-dashed lines and the residues involved in hydrophobic interactions are shown as red arcs. Hydrogen bonding and hydrophobic interactions were illustrated using LigPlot+ v.1.4.5 (Laskowski and Swindells, 2011).

References

Laskowski R A, Swindells M B (2011). LigPlot+: multiple ligand-protein interaction diagrams for drug discovery. J. Chem. Inf. Model., 51, 2778-2786.